Article

Opposed Steric Constraints in Human DNA Polymerase # and *E. coli* DNA Polymerase I

Francesca Di Pasquale, Daniela Fischer, Dina Grohmann, Tobias Restle, Armin Geyer, and Andreas Marx

J. Am. Chem. Soc., **2008**, 130 (32), 10748-10757 • DOI: 10.1021/ja8028284 • Publication Date (Web): 16 July 2008

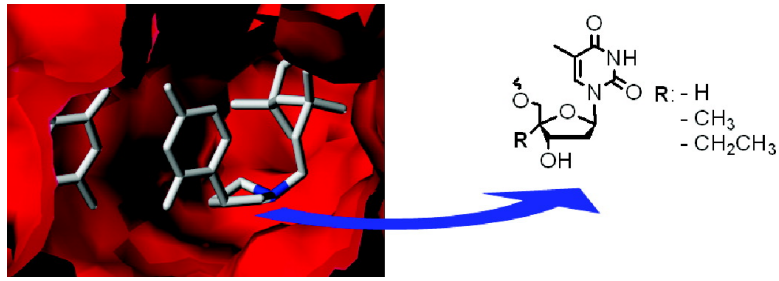

More About This Article

Additional resources and features associated with this article are available within the HTML version:

- Supporting Information
- Access to high resolution figures
- Links to articles and content related to this article
- Copyright permission to reproduce figures and/or text from this article

View the Full Text HTML

J|A|C|S
ARTICLES

Published on Web 07/16/2008

Opposed Steric Constraints in Human DNA Polymerase β and *E. coli* DNA Polymerase I

Francesca Di Pasquale,[†] Daniela Fischer,[§] Dina Grohmann,[||] Tobias Restle,[||] Armin Geyer,[‡] and Andreas Marx*,[†]

Fachbereich Chemie, Universität Konstanz, Universitätsstrasse 10, D-78457 Konstanz, Germany, Fachbereich Chemie, Hans Meerwein Strasse, Philipps-Universität Marburg, D-35032 Marburg, Germany, Institut für Organische Chemie, Universitätsstrasse 31, Universität Regensburg, D-93040 Regensburg, Germany, and Universitätsklinikum Schleswig-Holstein, Universität zu Lübeck, Institut für Molekulare Medizin, Ratzeburger Allee 160, D-23538 Lübeck, Germany

Received April 17, 2008; E-mail: andreas.marx@uni-konstanz.de

Abstract: DNA polymerase selectivity is crucial for the survival of any living species, yet varies significantly among different DNA polymerases. Errors within DNA polymerase-catalyzed DNA synthesis result from the insertion of noncanonical nucleotides and extension of misaligned DNA substrates. The substrate binding characteristics among DNA polymerases are believed to vary in properties such as shape and tightness of the binding pocket, which might account for the observed differences in fidelity. Here, we employed 4′-alkylated nucleotides and primer strands bearing 4′-alkylated nucleotides at the 3′-terminal position as steric probes to investigate differential active site properties of human DNA polymerase β (Pol β) and the 3′→5′-exonuclease-deficient Klenow fragment of *E. coli* DNA polymerase I (KF(exo-)). Transient kinetic measurements indicate that both enzymes vary significantly in active site tightness at both positions. While small 4′-methyl and -ethyl modifications of the nucleoside triphosphate perturb Pol β catalysis, extension of modified primer strands is only marginally affected. Just the opposite was observed for KF(exo-). Here, incorporation of the modified nucleotides is only slightly reduced, whereas size augmentation of the 3′-terminal nucleotide in the primer reduces the catalytic efficiency by more than 7000- and 260 000-fold, respectively. NMR studies support the notion that the observed effects derive from enzyme substrate interactions rather than inherent properties of the modified substrates. These findings are consistent with the observed differential capability of the investigated DNA polymerases in fidelity such as processing misaligned DNA substrates. The results presented provide direct evidence for the involvement of varied steric effects among different DNA polymerases on their fidelity.

Introduction

DNA polymerases catalyze all DNA synthesis in nature including DNA replication, repair, and recombination. They are template-depending enzymes that transfer the information of the parental strand to the daughter strand. Selectivity according to Watson−Crick nucleobase pairing in this process is crucial for the preservation of the integrity of every species genome. High-fidelity DNA polymerases involved in DNA replication exhibit intrinsic error rates as low as one error (i.e., incorporation of a non-Watson−Crick paired nucleotide) within 10^6 synthesized phosphodiester bonds.[1] However, certain DNA polymerases that are involved in DNA repair exhibit strikingly low fidelity when dealing with undamaged DNA.[1,2] An understanding of the basis for the striking differences in fidelity among DNA polymerases is essential to understand the process of DNA replication. However, the mechanistic origins of DNA polymerase selectivity are still a matter of debate.[3]

Errors within DNA polymerase-catalyzed DNA synthesis result from the insertion of noncanonical nucleotides and its subsequent extension leading to single nucleotide substitutions. Various models for nucleotide substitution fidelity have been suggested to describe the mechanisms of DNA polymerases to select the canonical nucleotide during the insertion steps.[1] At first glance, the formation of distinct hydrogen-bonding patterns between the nucleobases of the coding template strand and the incoming nucleoside triphosphate appears to be responsible for accurate nucleotide insertion. Yet, as suggested on the basis of thermal denaturating studies of matched and mismatched DNA complexes, these interactions alone are not sufficient to explain the extent of accuracy commonly observed for enzymatic DNA

[†] Universität Konstanz.
[‡] Philipps-Universität Marburg.
[§] Universität Regensburg.
[||] Universität zu Lübeck.

(1) (a) Echols, H.; Goodman, M. F. *Annu. Rev. Biochem.* **1991**, *60*, 477–511. (b) Kunkel, T. A.; Bebenek, K. *Annu. Rev. Biochem.* **2000**, *69*, 497–529. (c) Goodman, M. F. *Annu. Rev. Biochem.* **2002**, *71*, 17–50. (d) Kool, E. T. *Annu. Rev. Biochem.* **2002**, *71*, 191–219. (e) Kunkel, T. A. *J. Biol. Chem.* **2004**, *279*, 16859–16898. (f) Rothwell, P. J.; Waksman, G. *Adv. Protein Chem.* **2005**, *71*, 401–40. (g) McCulloch, S. D.; Kunkel, T. A. *Cell Res.* **2008**, *18*, 148–61.

(2) (a) Hübscher, U.; Maga, G.; Spadari, S. *Annu. Rev. Biochem.* **2002**, *71*, 133–163. (b) Prakash, S.; Johnson, R. E.; Prakash, L. *Annu. Rev. Biochem.* **2005**, *74*, 317–353.

(3) Kool, E. T.; Sintim, H. O. *Chem. Commun.* **2006**, *35*, 3665–3675.

10.1021/ja8028284 CCC: $40.75

synthesis.[1a,4] Extensive studies indicate that for some DNA polymerases hydrogen bonding alone is not strictly required to achieve high incorporation efficiencies.[1d,3] Close fitting of Watson−Crick geometry to the active site of the enzyme is cited as one of the most important factors for achieving selectivity in nucleotide insertion. However, DNA polymerase selectivity often varies significantly depending on the DNA polymerase.[1d,2] The origin of this varying error propensity is elusive. Variations of active sites "openness"[5] as well as their "tightness" [1d,6,7] are cited as cause for observed different selectivity.

Besides the occurrence of errors during the nucleotide insertion step, DNA polymerases often generate errors by deletion of a nucleotide or insertion of an additional nucleotide resulting in frameshift mutations.[1b,e,8] The mechanisms that govern these errors are less well understood than those of nucleotide substitution fidelity despite the fact that frameshift mutations might exhibit severe biological consequences.[8] Misalignment of the primer template complex is cited as reason for deletion and insertion errors.[1b,e,8] Recent studies have shown that strand misalignment fidelity depends on the DNA polymerase and varies more than 1000-fold.[8] For instance, human DNA polymerase β (Pol β), a member of the DNA polymerase family X, is much less accurate for single-nucleotide deletions than the 3′→5′-exonuclease-deficient Klenow fragment of *E. coli* DNA polymerase I (KF(exo-)), a member of the DNA polymerase family A.[9] As functional[10] and structural[11] studies indicate, DNA polymerases form complex interactions with the primer template and nucleotide substrates during catalysis of DNA polymerization that may reach up to several nucleotide pairs beyond the active site. These interactions primarily occur through the minor groove of the DNA duplex with the sugar−phosphodiester backbone and the nucleobases of the primer template complex. Structural studies indicate that Pol β undergoes fewer contacts with the DNA primer template duplex upstream of the active site compared to KF(exo-).[1b,12] These findings suggest that enzyme contacts with the primer template strands are crucial for misalignment fidelity. An enzyme exhibiting high misalignment fidelity might form tighter primer template binding pockets tolerating less geometric deviation (e.g., misaligned primer template complexes) and thereby preventing frameshift mutations resulting from nucleotide deletions and insertions, while low fidelity enzymes exhibit more flexibility leading to decreased fidelity. Indeed, recent studies of DNA polymerase λ, an enzyme belonging to the same family as Pol β that has a high single-base deletion error rate, have been shown to be sufficiently flexible to accommodate even an extrahelical nucleotide within the misaligned primer template complex.[13]

Recently, functional means to investigate steric constraints like "tightness" in DNA polymerases have been developed and yielded new insights into their function. Kool et al. have employed gradually expanding thymidine analogues to investigate tightness and polar effects within the active site acting on the nucleobase.[7] They used nonpolar nucleobase surrogates with a limited ability to form hydrogen bonds. Moreover, the size of these compounds increased incrementally by use of halogen atoms substituting the oxygen atoms of thymidine. We have developed and utilized 4′-alkyl-modified nucleotides, which continually increase in steric bulk for probing steric effects in DNA polymerase function acting on the deoxyribose.[6,10f,g] Alkyl groups were employed because potential effects on hydrogen-bonding patterns and conformations of the nucleotides on DNA polymerase function are minimized. Both approaches suggest an important contribution of steric effects on DNA polymerase selectivity and variations thereof to be involved in varied selectivity among different enzymes.

To better understand the fundamentals of markedly varied properties of DNA polymerases like Pol β and KF(exo-) (vide supra), we investigated the tightness of contacts of these

(4) Petruska, J.; Goodman, M. F.; Boosalis, M. S.; Sowers, L. C.; Cheong, C.; Tinoco, I., Jr *Proc. Natl. Acad. Sci. U.S.A.* **1988**, *85*, 6252–6256.
(5) (a) Silvian, L. F.; Toth, E. A.; Pham, P.; Goodman, M. F.; Ellenberger, T. *Nat. Struct. Biol.* **2001**, *8*, 984–989. (b) Trincao, J.; Johnson, R. E.; Escalante, C. R.; Prakash, S.; Prakash, L.; Aggarwal, A. K. *Mol. Cells* **2001**, *8*, 417–426. (c) Zhou, B. L.; Pata, J. D.; Steitz, T. A. *Mol. Cells* **2001**, *8*, 427–437. (d) Nair, D. T.; Johnson, R. E.; Prakash, S.; Prakash, L.; Aggarwal, A. K. *Nature* **2004**, *430*, 377–380. (e) Zang, H.; Goodenough, A. K.; Choi, J. Y.; Irimia, A.; Loukachevitch, L. V.; Kozekov, I. D.; Angel, K. C.; Rizzo, C. J.; Egli, M.; Guengerich, F. P. *J. Biol. Chem.* **2005**, *280*, 29750–29764. (f) Ling, H.; Boudsocq, F.; Woodgate, R.; Yang, W. *Cell* **2001**, *107*, 91–102. (g) Trincao, J.; Johnson, R. E.; Wolfle, W. T.; Escalante, C. R.; Prakash, S.; Prakash, L.; Aggarwal, A. K. *Nat. Struct. Mol. Biol.* **2004**, *11*, 457–462. (h) Ling, H.; Boudsocq, F.; Plosky, B. S.; Woodgate, R.; Yang, W. *Nature* **2003**, *424*, 1083–1087. (i) Ling, H.; Sayer, J. M.; Plosky, B. S.; Yagi, H.; Boudsocq, F.; Woodgate, R.; Jerina, D. M.; Yang, W. *Proc. Natl. Acad. Sci. U.S.A.* **2004**, *101*, 2265–2269.
(6) (a) Summerer, D.; Marx, A. *Angew. Chem., Int. Ed.* **2001**, *40*, 3693–3695. (b) Strerath, M.; Summerer, D.; Marx, A. *ChemBioChem* **2002**, *3*, 578–580. (c) Strerath, M.; Cramer, J.; Restle, T.; Marx, A. *J. Am. Chem. Soc.* **2002**, *124*, 11230–11231. (d) Cramer, J.; Strerath, M.; Marx, A.; Restle, T. *J. Biol. Chem.* **2002**, *277*, 43593–43598. (e) Cramer, J.; Rangam, G.; Marx, A.; Restle, T. *ChemBioChem* **2008**, *9*, 1243–1250.
(7) (a) Kim, T. W.; Delaney, J. C.; Essigmann, J. M.; Kool, E. T. *Proc. Natl. Acad. Sci. U.S.A.* **2005**, *102*, 15803–15808. (b) Mizukami, S.; Kim, T. W.; Helquist, S. A.; Kool, E. T. *Biochemistry* **2006**, *45*, 2772–2778. (c) Kim, T. W.; Brieba, L. G.; Ellenberger, T.; Kool, E. T. *J. Biol. Chem.* **2006**, *281*, 2289–2295. (d) Sintim, H. O.; Kool, E. T. *J. Am. Chem. Soc.* **2006**, *128*, 396–397. (e) Sintim, H. O.; Kool, E. T. *Angew. Chem., Int. Ed.* **2006**, *45*, 1974–1979. (f) Silverman, A. P.; Jiang, Q.; Goodman, M. F.; Kool, E. T. *Biochemistry* **2007**, *46*, 13874–13881.
(8) Garcia-Diaz, M.; Kunkel, T. A. *Trends Biochem. Sci.* **2006**, *31*, 206–14.
(9) (a) Kunkel, T. A. *Biochemistry* **1990**, *29*, 8003–8011. (b) Bebenek, K.; Joyce, C. M.; Fitzgerald, M. P.; Kunkel, T. A. *J. Biol. Chem.* **1990**, *265*, 13878–13887. (c) Osheroff, W. P.; Jung, H. K.; Beard, W. A.; Wilson, S. H.; Kunkel, T. A. *J. Biol. Chem.* **1999**, *274*, 3642–3650.
(10) (a) Carver, T. E., Jr.; Hochstrasser, R. A.; Millar, D. P. *Proc. Natl. Acad. Sci. U.S.A.* **1994**, *91*, 10670–10674. (b) Morales, J. C.; Kool, E. T. *J. Am. Chem. Soc.* **1999**, *121*, 2323–2324. (c) Morales, J. C.; Kool, E. T. *Biochemistry* **2000**, *39*, 12979. (d) Spratt, T. E. *Biochemistry* **2001**, *40*, 2647–2652. (e) Thompson, E. H. Z.; Bailey, M. F.; van der Schans, E. J. C.; Joyce, C. M.; Millar, D. P. *Biochemistry* **2002**, *41*, 713–722. (f) Summerer, D.; Marx, A. *J. Am. Chem. Soc.* **2002**, *124*, 910–911. (g) Strerath, M.; Gaster, J.; Marx, A. *ChemBioChem* **2004**, *5*, 1585–1588.
(11) For example:(a) Pelletier, H.; Sawaya, M. R.; Kumar, A.; Wilson, S. H.; Kraut, J. *Science* **1994**, *264*, 1891–1903. (b) Doublié, S.; Tabor, S.; Long, A. M.; Richardson, C. C.; Ellenberger, T. *Nature* **1998**, *391*, 251–258. (c) Li, Y.; Korolev, S.; Waksman, G. *EMBO J.* **1998**, *17*, 7514–7525. (d) Kiefer, J. R.; Mao, C.; Braman, J. C.; Beese, L. S. *Nature* **1998**, *391*, 304–307. (e) Huang, H. F.; Chopra, R.; Verdine, G. L.; Harrison, S. C. *Science* **1998**, *282*, 1669–1675. (f) Franklin, M. C.; Wang, J.; Steitz, T. A. *Cell* **2001**, *105*, 657–667. (g) Johnson, S. J.; Taylor, J. S.; Beese, L. S. *Proc. Natl. Acad. Sci. U.S.A.* **2003**, *100*, 3895–3900. (h) Johnson, S. J.; Beese, L. S. *Cell* **2004**, *116*, 803–816. (i) Kamtekar, S.; Berman, A. J.; Wang, J.; Lázaro, J. M.; de Vega, M.; Blanco, L.; Salas, M.; Steitz, T. A. *EMBO J.* **2006**, *25*, 1335–1343. (j) Berman, A. J.; Kamtekar, S.; Goodman, J. L.; Lázaro, J. M.; de Vega, M.; Blanco, L.; Salas, M.; Steitz, T. A. *EMBO J.* **2007**, *26*, 3494–3505.
(12) Beard, W. A.; Wilson, S. H. *Chem. Rev.* **2006**, *106*, 361–382.
(13) (a) Garcia-Diaz, M.; Bebenek, K; Krahn, J. M.; Pedersen, L. C.; Kunkel, T. A. *Cell* **2006**, *124*, 331–342. (b) Bebenek, K.; Garcia-Diaz, M.; Foley, M. C.; Pedersen, L. C.; Schlick, T.; Kunkel, T. A. *EMBO Rep.* **2008**, *9*, 459–64.

enzymes with their substrates. We employed 4′-alkylated nucleotides and oligonucleotides as steric probes and compared active site constraints acting on the nucleoside triphosphate as well as on the primer template of the respective enzyme. Depending on the position of the steric probe (incoming nucleotide or 3′-end of the primer strand) and the enzyme studied, drastically different effects concerning nucleotide incorporation were observed. Comparative NMR investigations of 4′-modified oligonucleotides and nonmodified counterparts indicated no significant effect of the modification on DNA conformation and duplex formation. Thus, this finding supports the notion that the observed effects derive from size augmentation of the substrate rather than the formation of aberrant substrate conformations. Our findings strongly indicate that indeed these varied size constraints are accountable for the observed differences in substrate recognition accuracy of Pol β and KF(exo-).

Materials and Methods

Purification of Recombinant DNA Polymerases. A 3′−5′-exonuclease-deficient variant of the Klenow Fragment of *E. coli* DNA polymerase I and human DNA polymerase β were expressed and purified as described.[14] The purity of the proteins was >95% as controlled by SDS-PAGE. The concentrations were determined by the Bradford assay.

Nucleoside Triphosphates and DNA Substrates. 4′-Modified nucleoside triphosphates and oligonucleotides were synthesized and purified as described.[6,10f,g] Unmodified dNTPs were purchased from Roche. Unmodified oligonucleotides were purchased from IBA, Göttingen. Employed sequences: primer 24merA, 5′-d(GTG GTG CGA AAT TTC TGA CAG ACA); primer 25merT^{R}, 5′-d(GTG GTG CGA AAT TTC TGA CAG ACA **T^{R}**, R: **H** = 4′-H, **Me** = 4′-CH_3, **Et** = 4′-CH_2CH_3; template 36mer, 5′-d(GTG CGT CTG TCA TGT CTG TCA GAA ATT TCG CAC CAC). The primer strands were radiolabeled using γ-[^{32}P]-ATP and T4 polynucleotide kinase (Fermentas) according to standard protocols.

Primer Extension Studies. Pol β reactions contained 40 nM primer template and 40 nM enzyme in 50 mM TrisHCl pH 8.0, 10 mM $MgCl_2$, 2 mM DTT, 20 mM NaCl, 20 mM KCl, 200 μg/mL BSA, glycerol 1%[15] in a final volume of 20 μL and dNTPs at the concentrations indicated in the corresponding figures. KF(exo-) reaction mixtures consisted of 40 nM primer template and 2 nM enzyme in 50 mM TrisHCl pH 7.3, 10 mM $MgCl_2$, 1 mM DTT[6a] in a final volume of 20 μL and dNTPs at the concentrations indicated in the corresponding figures. The reaction mixtures were incubated for 20 min at 37 °C and subsequently quenched using PAGE loading solution (80% [v/v] formamide, 20 mM EDTA, 0.025% [w/v] bromophenol blue, 0.025% [w/v] xylene cyanol) and analyzed by 12% PAGE containing 8 M urea. Visualization was performed using phosphorimaging.

Kinetics. The rate of single turnover, single nucleotide incorporation was determined using the different primer/36mer template DNA duplexes performing presteady-state measurements. Rapid-quench assays were carried out using a KinTek RQF-3 rapid quench flow apparatus (KinTek Corp., Austin, TX). Pol β reaction mixtures contained 100 nM primer template, 1 μM enzyme, and different concentrations of dNTP in reaction buffer. KF(exo-) reaction mixtures consisted of 100 nM primer template, 200 nM enzyme, and different concentrations of dNTP in reaction buffer. The reaction was initiated by mixing equal volumes (15 μL each) of a solution containing enzyme and DNA primer template substrate with a solution containing the dNTP (0.1 μM−1 mM) in reaction buffer. For reaction times ranging from 0.05 to 10 s, the rapid quench instrument was used. The reactions were quenched using 0.6% TFA prior to mixing with a PAGE loading solution (80% [v/v] formamide, 0.025% [w/v] bromophenol blue, 0.025% [w/v] xylene cyanol). For reaction times longer than 10 s, a manual quench was performed. Samples of the quenched reactions were denatured at 95 °C for 5 min and analyzed by 12% PAGE containing 8 M urea. Visualization was carried out by phosphorimaging. The product bands were quantified using the BioRad Quantity One software. For presteady-state analysis, experimental data were fit by nonlinear regression using the program GraphPad Prism 4. The data were fit to a single exponential equation: [Primer + 1] = A*(1 − exp(−$k_{obs}t$)). The observed catalytic rates (k_{obs}) were then plotted against the dNTP concentration used, and the data were fitted to a hyperbolic equation to determine the K_d of the incoming nucleotide. The incorporation efficiency is given by k_{pol}/K_d. The kinetic data result from multiple independently conducted experiments (duplicates or triplicates).

NMR Studies. The signal assignment for the tetramers dACAT (**4PH**) (1.6 mg, $n = 1.09 \times 10^{-6}$ mol, $c = 1.66$ mM), dACAT^{Me} (**4PM**) (1.84 mg, $n = 1.25 \times 10^{-6}$ mol, $c = 1.79$ mM), and dATGT (**4T**) (3.42 mg, $n = 2.29 \times 10^{-6}$ mol, $c = 3.27$ mM) were performed as triethylammonium salts at 300 K in 0.7 mL in phosphate buffer (30 mM, pH 7, D_2O). The double strands **4PM**/**4T** and **4PH**/**4T** were obtained by adding **4T** to the NMR tubes containing **4PM** (455 μL of **4T**, molar ratio **4PH**:**4T** = 0.95) and **4PH** (515 μL, molar ratio **4PM**:**4T** = 0.96), respectively. All measurements were performed on a Bruker Avance DRX 600 spectrometer with a 5 mm BBI probe head. Homonuclear 2D spectra (TOCSY, ROESY) were recorded at 320 K in the phase-sensitive mode as data matrices of 512 (t_1) real × 2048 (t_2) complex data points; 48 scans (TOCSY) and 80 scans, respectively, were used per t_1 increment. The used spectral widths were between 6602 and 9014 Hz. Mixing times of 100 ms (TOCSY) and 150 ms (ROESY) were applied. Heteronuclear 2D HSQC experiments were performed in the phase-sensitive mode with data matrices of 512 (t_1, ^{13}C) real × 2048 (t_2, ^{1}H) complex data points and 80 scans per t_1 increment. All data were recorded and analyzed using Bruker TopSpin software. This chemical shift is calibrated on sodium 3-(trimethylsilyl)propionic acid (δ = 0.00 ppm, ^{1}H) and acetate as internal references (δ = 21.03 ppm, ^{13}C), respectively.

Results

Primer Extension by Pol β and KF(exo-). To probe the active sites and primer contacts of Pol β and KF(exo-), we performed single nucleotide incorporation studies employing a radiometric assay (Figure 1). First, we investigated incorporation of thymidine and the size augmented steric probes derived by substitution of the 4′-hydrogen atom with methyl and ethyl, respectively. Under the chosen conditions, Pol β did not incorporate size augmented thymidine analogues, while the unmodified TTP was processed (Figure 1C). In contrast, KF(exo-) accepted the steric probes, and primer extension was observed in all cases (Figure 1C). However, when primer extension from the size augmented nucleotides placed at the 3′-terminal nucleotide in the primer strand was investigated, opposed results were observed for both enzymes (Figure 1D). Pol β was able to extend 4′-alkylated primer strands to a certain extent, while KF(exo-) was unable to synthesize significant amounts of extension products. These observations indicate that significantly different steric constraints act on the incoming nucleotide and the primer strand of the two polymerases, which were quantified as described in the following.

Quantitative Studies of Pol β. To characterize the active site tightness of Pol β in more detail, we measured nucleotide incorporation under presteady-state conditions using a quench flow device. Kinetic experiments were performed by examining

(14) (a) Summerer, D.; Rudinger, N. Z.; Detmer, I.; Marx, A. *Angew. Chem., Int. Ed.* **2005**, *44*, 4712–4715. (b) Kosa, J. L.; Sweasy, J. B. *J. Biol. Chem.* **1999**, *274*, 3851–3858.

(15) Tae, E. L.; Wu, Y.; Xia, G.; Schultz, P. G.; Romesberg, F. E. *J. Am. Chem. Soc.* **2001**, *123*, 7439–40.

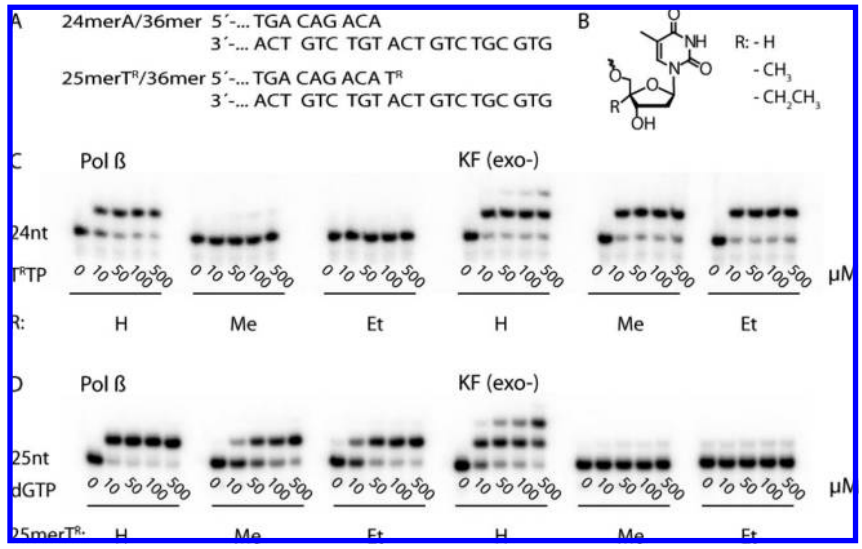

Figure 1. Effects of 4′-alkyl groups on Pol β and KF(exo-) promoted nucleotide insertion. (A) Partial DNA sequences and (B) thymidine analogues used in this study. (C) Effects on incoming nucleotide. (D) Effects on 3′-terminal position in primer strand; dNTP concentrations are indicated in the figure. Reactions performed at 37 °C for 20 min equally contained Pol β or KF(exo-) and primer template complex.

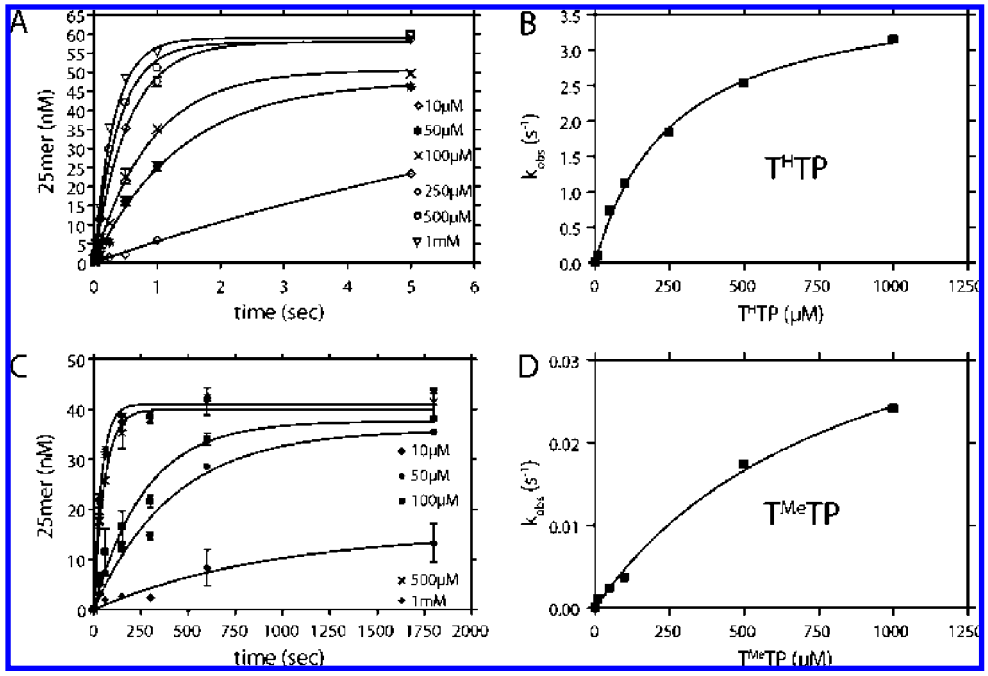

Figure 2. Presteady-state kinetics of $T^{H}TP$ and $T^{Me}TP$ incorporation into 24mer/36mer primer template complex (100 nM) by Pol β (1 μM). (A and C) Product versus time plot. The curves show the best fit of the data to a single exponential equation. A preformed complex of Pol β and primer template was rapidly mixed with different concentrations of $T^{H}TP$ (A) or $T^{Me}TP$ (C) as indicated in the figure. (B and D) Dependence of the presteady-state rates on the $T^{H}TP$ (B) or $T^{Me}TP$ (D) concentration. The k_{obs} values were plotted versus the $T^{R}TP$ concentration and fitted to a hyperbolic equation.

single nucleotide extensions of a 24mer primer annealed to a 36mer template using an excess of enzyme over DNA substrate (Figure 2). The resulting values of k_{pol}, that is, effective presteady-state nucleotide incorporation rate, K_d, which is the affinity of the binary polymerase/primer template complex for the incoming nucleotide, and the incorporation efficiency (k_{pol}/K_d) are listed in Table 1. For the unmodified $T^{H}TP$, a K_d of 264 ± 24 μM and a polymerization rate of 3.9 ± 0.1 s^{-1} were found. These results are in the same order as recently published data obtained in a different sequence context.[16] Binding of $T^{Me}TP$ was about 3-fold weaker as compared to the unmodified substrate, and the incorporation rate dropped about 100-fold. Together, this yielded a 280-fold decrease of nucleotide incorporation efficiency through size augmentation by a methylene group. Further increasing the size of the modified substrate by an ethyl group was not tolerated by Pol β, and nucleotide insertion was not observed even at high concentrations of $T^{Et}TP$ (up to 2 mM). To determine possible steric constraints acting on the primer strand, the 3′-end of the primer was modified with a $T^{R}MP$ residue and elongation by Pol β was analyzed. For this endeavor, we used a 25mer primer strand annealed to a 36mer template used before. Primer extension by incorporation

(16) Werneburg, B. G.; Ahn, J.; Zhong, X.; Hondal, R. J.; Kraynov, V. S.; Tsai, M. D. *Biochemistry* **1996**, *35*, 7041–50.

Table 1. Kinetic Parameters for the Incorporation of T^{R}TP Using a 24nt Primer 36nt Template[a]

	K_d (μM)		k_{pol} (s^{-1})		k_{pol}/K_d (M^{-1} s^{-1})	
	Pol β	KF(exo-)	Pol β	KF(exo-)	Pol β	KF(exo-)
R = H	264 ± 24	33 ± 1.0	3.9 ± 0.1	230 ± 13	15 000	7 000 000
R = Me	870 ± 197	44 ± 6.0	0.046 ± 0.006	5.7 ± 0.4	53	130 000
R = Et	n.a.	53 ± 4.9	n.a.	3.2 ± 0.1	n.a.	60 000

[a] n.a., not accessible.

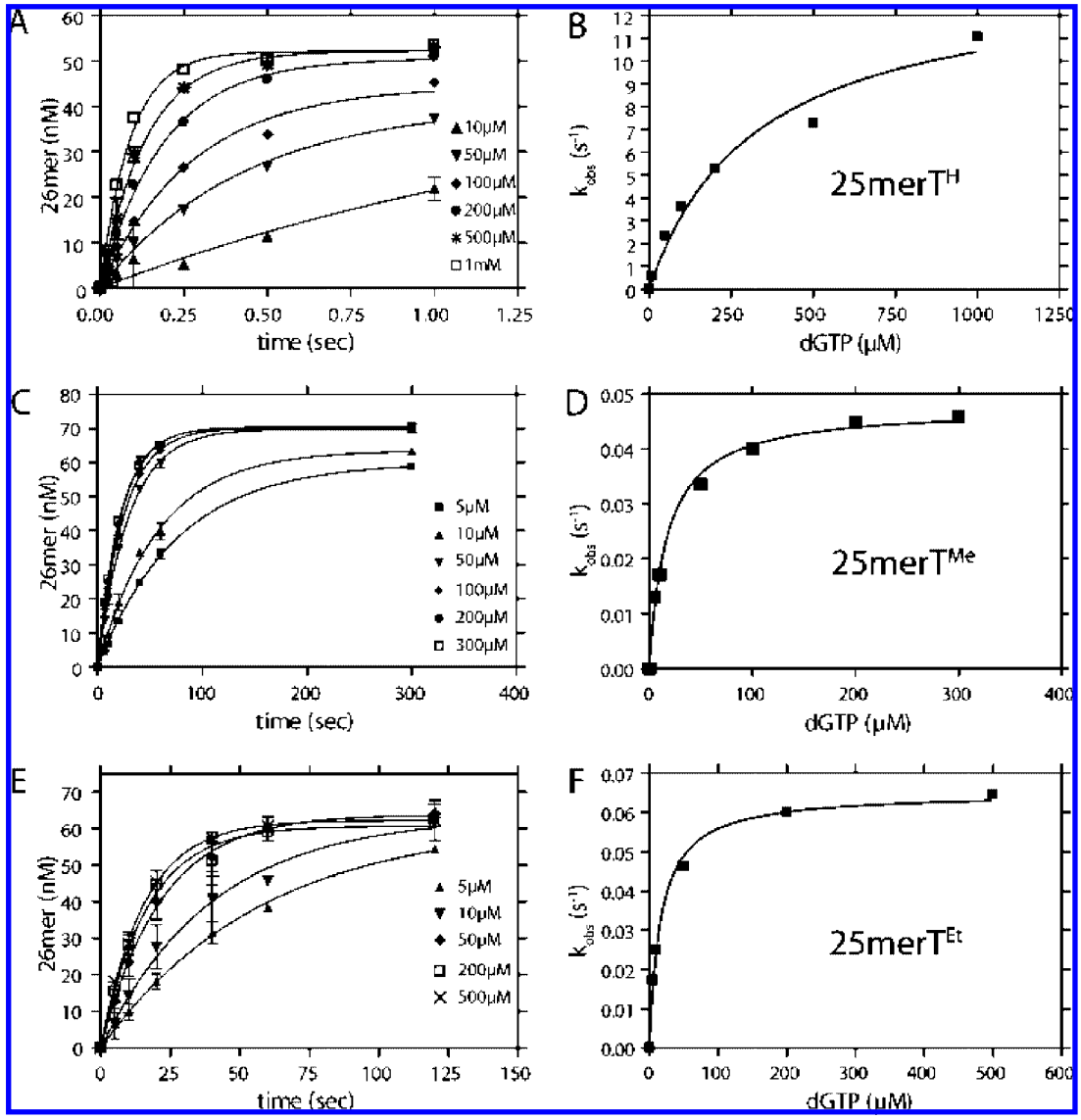

Figure 3. Presteady-state kinetics of single nucleotide (dG) extension of a 25merT^{R}/36mer primer template complexes (100 nM) by Pol β (1 μM). (A,C,E) Product versus time plots. The curves show the best fit of the data to a single exponential equation. A preformed complex of Pol β and 25merT^{R}/36mer primer template was rapidly mixed with different concentrations of dGTP as indicated in the figure. (B,D,F) Dependence of the observed presteady-state rates on dGTP concentration. The k_{obs} values were plotted versus the concentration of dGTP and fitted to a hyperbolic equation.

Table 2. Kinetic Parameters for the Incorporation of dGTP Using 4′-Alkylated 25merT^{R} Primer 36mer Template

	K_d (μM)		k_{pol} (s^{-1})		k_{pol}/K_d (M^{-1} s^{-1})	
	Pol β	KF(exo-)	Pol β	KF(exo-)	Polβ	KF(exo-)
25merT^{H}	328 ± 85	1.6 ± 0.2[a]	13.8 ± 1.5	20.0 ± 0.3[a]	42 000	12 000 000[a]
25merT^{Me}	17.3 ± 2.3	10.2 ± 1.8	0.048 ± 0.001	0.017 ± 0.001	2800	1700
25merT^{Et}	16.4 ± 2.0	16.7 ± 1.8	0.065 ± 0.018	0.00076 ± 0.00002	4000	45

[a] Reaction performed at 22 °C.

of a canonical dGTP opposite a dC in the template was investigated (Figure 3, Table 2). Pol β showed a K_d of 328 ± 85 μM for dGTP and an incorporation rate of 13.8 ± 1.5 s^{-1} when an unmodified primer template complex was used. Primer extension was hampered by 4′-alkylation and decreased about 15-fold when extending from 25merT^{Me} and 10-fold from

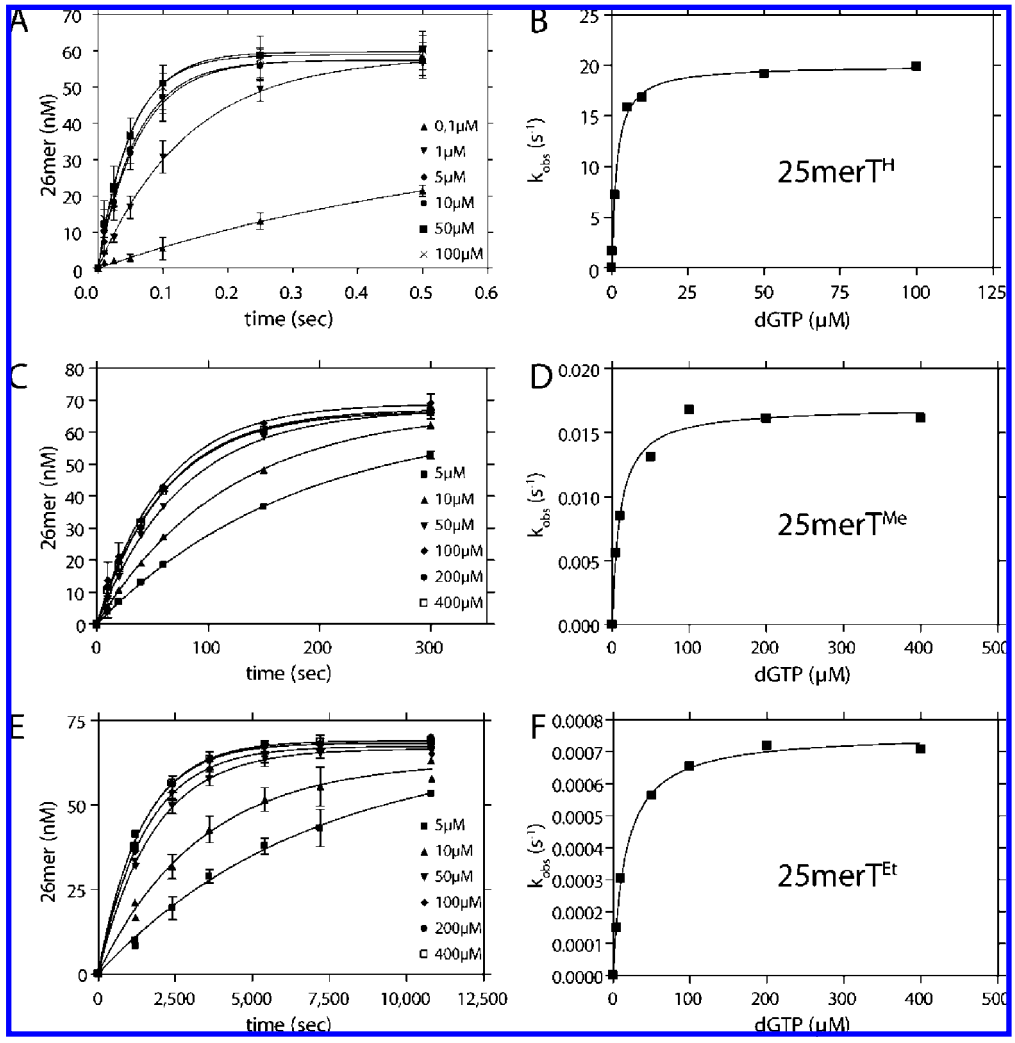

Figure 4. Presteady-state kinetics of single nucleotide (dG) extension of a 25merT^{R}/36mer primer template complexes (100 nM) by KF(exo-) (200 nM). (A,C,E) Product versus time plots. The curves show the best fit of the data to a single exponential equation. A preformed complex of KF(exo-) and 25merT^{R}/36mer primer template was rapidly mixed with different concentrations of dGTP as indicated in the figure. (B,D,F) Dependence of the observed presteady-state rates on dGTP concentration. The k_{obs} values were plotted versus the concentration of dGTP and fitted to a hyperbolic equation.

25merT^{Et}. Albeit size augmentation at the primer through 4′-alkylation of the terminal nucleotide had effects on extension efficiency of Pol β, the observed effects of the modifications are less pronounced as compared to the effects of steric constraints acting on the incoming nucleotide.

Quantitative Studies of KF(exo-). As we reported recently,[6e] KF(exo-) showed a higher incorporation efficiency using steric augmented analogues of T^{H}TP as compared to Pol β (Table 1). However, as shown in the present study, elongation of primers bearing a modified T^{R}MP at the 3′-end was significantly affected. While the recently reported T^{R}TP incorporation studies were conducted employing transient kinetics,[6e] extension studies from modified primer strands shown in Figure 1 were performed by steady-state kinetic analysis.[10f] To directly compare the Pol β data with KF(exo-) data, we additionally did a transient kinetic analysis of KF(exo-), performing extension studies from 3′-terminal nonmodified and 4′-modified primers using the same oligonucleotide sequences as before. Our results employing unmodified substrates are within the same order as recently published data obtained in a different sequence context,[17] whereas the affinity of a binary complex of KF(exo^{-}) and the 4′-modified primer template complex for dGTP decreased by a factor of 10 (Figure 4, Table 2). Most interestingly, a dramatic drop in nucleotide incorporation rates was observed with the 4′-methyl-substituted primer. Here, the polymerization rate of the enzyme dropped more than 1000-fold and for the 4′-ethyl-substituted primer more than 26 000-fold. This resulted in 7000- and 260 000-fold declines of extension efficiency, respectively. Taken together, KF(exo-) is significantly more sensitive to 4′-alkyl modifications at the primer strand and thus exhibits an opposed behavior to Pol β (Figure 5).

NMR Studies. The observed effects might well derive from aberrant oligonucleotide conformations at the primer end caused by the 4′-modifications. Up to now, 4′-modified oligonucleotides were investigated by employment of CD spectroscopy.[18] To gain more insights in whether 4′-modifications at the 3′-primer end might have an effect on the DNA conformation, we performed NMR studies. Because ^{1}H chemical shifts, *J*-couplings, and NOEs are sensitive to variations of DNA conformational

(17) (a) Kuchta, R. D.; Mizrahi, V.; Benkovic, P. A.; Johnson, K. A.; Benkovic, S. J. *Biochemistry* **1987**, *26*, 8410–8417. (b) Lowe, L. G.; Guengerich, F. P. *Biochemistry* **1996**, *35*, 9840–9849. (c) Astatke, M.; Grindley, N. D.; Joyce, C. M. *J. Mol. Biol.* **1998**, *278*, 147–165.

(18) (a) Detmer, I.; Summerer, D.; Marx, A. *Eur. J. Org. Chem.* **2003**, 1837–1846. (b) Detmer, I.; Summerer, D.; Marx, A. *Chem. Commun.* **2002**, 2314–2315.

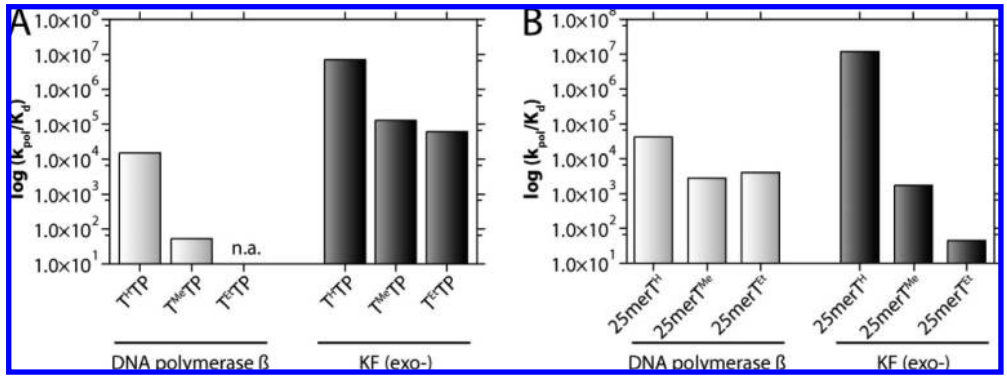

Figure 5. (A) Representation of the incorporation efficiencies of T^RTP into a 24nt/36nt primer template by Pol β and KF(exo-). (B) Representation of the incorporation efficiencies of dGTP into 4′-alkylated 25ntT^R/36nt primer template complexes by Pol β and KF(exo-).

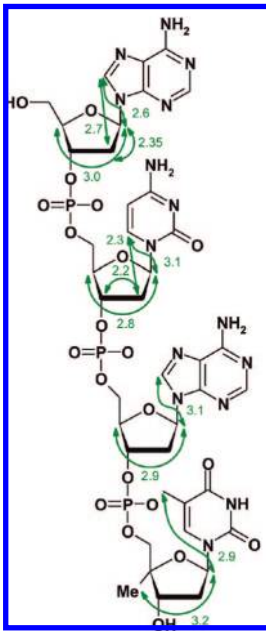

ROE	Experimental distances [Å]	Sequential ROEs in B-DNA (C2′-endo, anti) [Å]
H2′a – H5b	3.55	3.6
H2″a – H5b	**4.1**	**2.7**
H2″a – H6b	**3.2**	**2.2**
H2′b – H8c	3.9	3.8
H2″b – H8c	**3.4**	**2.1**
H3′b – H8c	3.3	4.6
H1′c – H7d(Me)	4.0	> 4.5
H3′c – H7d(Me)	**3.2**	**> 4.5**
H4′c – H7d(Me)	3.8	> 4.5
H8c – H7d(Me)	3.7	3.8

Figure 6. Average ROE-derived distances within nucleotides a, b, c, and d of **4PM** (green arrows) identify the syn/anti ratio and the ring puckering. Sequential ROEs between neighboring nucleotides of **4PM** are listed in the table together with the average interproton distances of C2′-*endo* ring puckers of B-DNA. Bold values highlight significant differences between **4PM** and the values expected for idealized B-DNA.

equilibriums, NMR spectroscopy can identify local properties like ring puckering or the syn/anti equilibriums of bases as well as global changes like the melting temperature of double-stranded DNA. Here, we performed for the first time structural analysis of a 4′-methylated nucleotide incorporated in an oligonucleotide and in the presence of the complementary strand. Two complementary tetrameric DNA strands in the same sequence context were chosen as structural model for the dynamic behavior of the fraying ends of a DNA double-strand. We synthesized and compared a 4′-methylated oligonucleotide $dACAT^{Me}$ (**4PM**), with its unmodified counterpart **4PH** with and without the complementary strand, respectively. All signal assignments are based on homo- and heteronuclear NMR spectra. By rotating-frame NOEs (ROEs), neighboring nucleotides were identified, which allowed sequential analysis. Additionally, time-averaged interproton distances were obtained according to Wüthrich.[19] First, the single strands **4PH** and **4PM** were investigated (Figure 6). Deoxyriboses adopt mainly 2′-endo puckering and are averaged in syn/anti equilibria except for the 5′-terminal adenosine, which is found in the syn-orientation. Thus, 4′-methylation neither significantly alters the ring puckering or the base orientation of the nucleotide itself nor does it influence the conformational behavior of neighboring nucleotides in single-stranded DNA.

Addition of the complementary strand **4T** to **4PH** and **4PM**, respectively, identified the differences and similarities in the pairing behavior of the oligonucleotides. In both cases, the same nucleobase protons experience chemical shift differences, but there was no detectable influence of 4′-alkylation on the complementary oligonucleotide. Chemical shift variations of both adenines of **4PM** are explained by minimal variations of the base orientations, yet too small to result in variations of the ROE pattern at 300 K, and an overlay of the ROESY spectra of **4PM** and **4PH** shows only minimal differences (Figure 7, Table 3). As for the single strands, the syn/anti equilibrium of the nucleobases contributed significantly to time-averaging of ROEs. The temperature dependence of the mixtures **4T/4PH** and **4T/4PM**, respectively, between 275 and 300 K showed duplex formation over a wide temperature range (data not shown). Both minimal DNA **4PH** and **4PM** exhibit nearly the

(19) Wüthrich, K. *NMR of Proteins and Nucleic Acids*; J. Wiley & Sons: New York, 1986; pp 220−222.

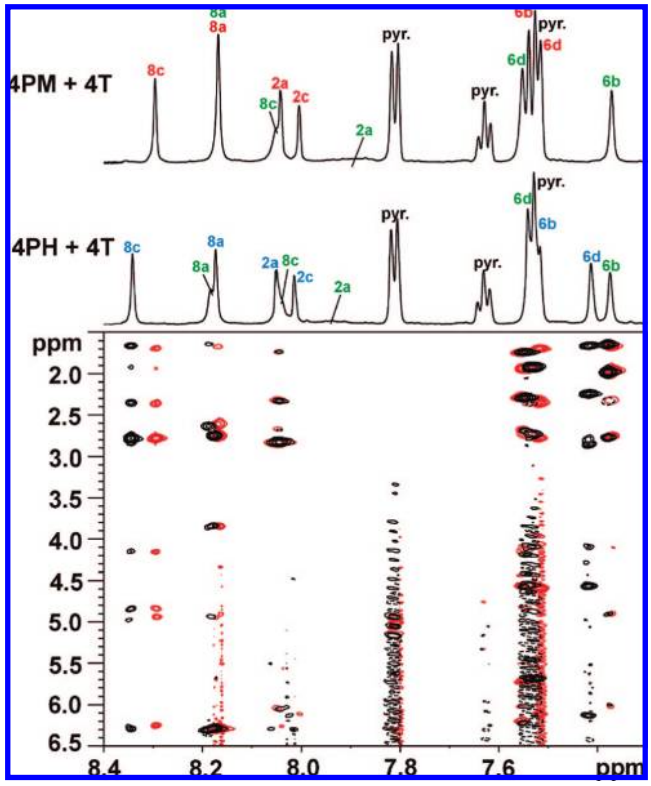

Figure 7. ROESY expansion (600 MHz, 277 K) for the base resonances of **4PH/4T** and **4PM/4T** together with the ^{1}H NMR projections.

same behavior in the presence of the complementary strand **4T**, and there is again, as already described for the single strands, no detectable influence of 4′-methylation on the *J* coupling pattern. Yet, differences of up to 0.5 Å are observed for the average ROE distances between sugar protons and the nucleobase for all four nucleotides. This can be explained by variations of the syn/anti equilibria. While the 3′-terminal nucleotide of **4PH** and **4PM**, which is the site of 4′-methylation, exhibits similar averaged ROEs due to the syn/anti equilibriums of the nucleobase, the neighboring adenine syn/anti equilibrium is slightly shifted toward syn in **4PM**. In conclusion, the overall influence of 4′-methylation on the conformational equilibrium of oligonucleotides is surprisingly small.

Discussion

Our kinetic investigations of Pol β and KF(exo-) indicate considerably different steric constraints, which act on the sugar backbone of the incoming nucleotide within the active site and the 3′-end of the primer strand. In all cases, the major effects of alkyl substitutions were found in the k_{pol} term and only to a lesser extent in the K_d term. This indicates that the steps leading to nucleotide incorporation (e.g., conformational enzyme changes and/or phosphodiester bond formation) are more affected by size augmentation than the initial binding step. Interestingly, in case of two DNA polymerases investigated, the effects on reactivity by size augmented nucleotides are directly opposed (Figure 5). Albeit size augmentation by 4′-alkylation of the nucleoside triphosphate substrate affects incorporation efficiency of both enzymes, the effects on Pol β are significantly more pronounced as compared to KF(exo-). In particular, expanding the size by one additional methylene group from 4′-methylation to 4′-ethylation is well tolerated by KF(exo-) and resulted only in a further 2-fold reduction of incorporation efficiency, while the larger nucleotide was no substrate for Pol β. These results can be rationalized by differential steric demand of the nascent base within the active site of the two DNA polymerases.

Table 3. $^3J_{HH}$ Coupling within the Deoxyribose Rings of **4PH** and **4PM** Bound to the Complementary DNA Strand

	$^3J_{HH}$ [Hz]				
	4PH	4PM		4PH	4PM
a-ring			b-ring		
H1′−H2′	8	8	H1′−H2′	8	8
H1′−H2″	6	6	H1′−H2″	6	6
H2′−H3′	6	6	H2′−H3′	6	6
H2″−H3′	3	3	H2″−H3′	3	2
H3′−H4′	3	3	H3′−H4′	3	3
c-ring			d-ring		
H1′−H2′/H2″	6/7.5	7/7	H1′−H2′/H2″	7/7	6.5/6.5
H2′/H2″−H3′	3/6	3/n.d.	H2′/H2″−H3′	−/6.5	−/7
H3′−H4′	3	3	H3′−H4′	4	

For Pol β, crystal structures of the ternary complex (i.e., enzyme, primer template, and incoming dNTP) are available.[11a,12,20] Given that there is no structural information existing for KF(exo-) highly homologous *Bacillus stearothermophilus* DNA polymerase I (Bst Pol)[11d,g,h] is often used to correlate functional data to KF(exo-) structure. The available structures reveal that the deoxyribose moiety of the incoming dNTP is fully embedded within the substrate binding pockets of these DNA polymerases and is an integral part of the substrate recognition processes (Figure 8). The Bst Pol structure indicates that the sugar of the incoming dNTP has contacts with various residues, Arg615, Ile657, Glu658, and Asp830 (the corresponding residues in KF(exo-) are Arg668, Ile709, Glu710, and Asp830). Mutational studies of KF(exo-) showed that these residues affect fidelity.[1b,21] Moreover, structural data reveal that Tyr271 and Phe272 in α-helix M of Pol β are located in the near proximity of the sugar moiety of the incoming nucleotide. These interactions in Pol β have been discussed to be involved in the discrimination of mismatches as well.[1b] Thus, editing of the incoming dNTP sugar residue might provide DNA polymerases with an additional option to achieve canonical base pair formation through indirect readout of aberrant sugar conformations. Indeed, structural analysis of Bst Pol[11h] and Pol β[20] complexed with noncanonical substrates as well as modeling studies of Pol β[22] suggest significantly altered protein side chain and nucleotide conformations as compared to the structures obtained from fully canonical substrates. Furthermore, it was reported in studies of related DNA polymerases that size alteration of amino acids that contact the nucleotide sugar residues may lead to altered enzyme fidelity.[1b,23] This observation further supports the notion that at least for the investigated enzymes, the recognition of the 2′-deoxyribose unit is an integral part of DNA polymerase selectivity mechanism.

(20) (a) Pelletier, H.; Sawaya, M. R.; Kumar, A.; Wilson, S. H.; Kraut, J. *Science* **1994**, *264*, 1891. (b) Sawaya, M. R.; Prasad, P.; Wilson, S. H.; Kraut, J.; Pelletier, H. *Biochemistry* **1997**, *36*, 11205. (c) Batra, V. K.; Beard, W. A.; Shock, D. D.; Krahn, J. M.; Pedersen, L. C.; Wilson, S. H. *Structure* **2006**, *14*, 757.

(21) Minnick, D. T.; Bebenek, K.; Osheroff, W. P.; Turner, R. M., Jr.; Astatke, M.; Liu, L.; Kunkel, T. A.; Joyce, C. M. *J. Biol. Chem.* **1999**, *274*, 3067–3075.

(22) (a) Alberts, I. L.; Wang, Y; Schlick, T. *J. Am. Chem. Soc.* **2007**, *129*, 11100–10. (b) Radhakrishnan, R.; Arora, K.; Wang, Y.; Beard, W. A.; Wilson, S. H.; Schlick, T. *Biochemistry* **2006**, *45*, 15142–56. (c) Arora, K; Beard, W. A.; Wilson, S. H.; Schlick, T. *Biochemistry* **2005**, *44*, 13328–41. (d) Radhakrishnan, R.; Schlick, T. *J. Am. Chem. Soc.* **2005**, *127*, 13245–52. (e) Radhakrishnan, R.; Schlick, T. *Proc. Natl. Acad. Sci. U.S.A.* **2004**, *101*, 5970–5.

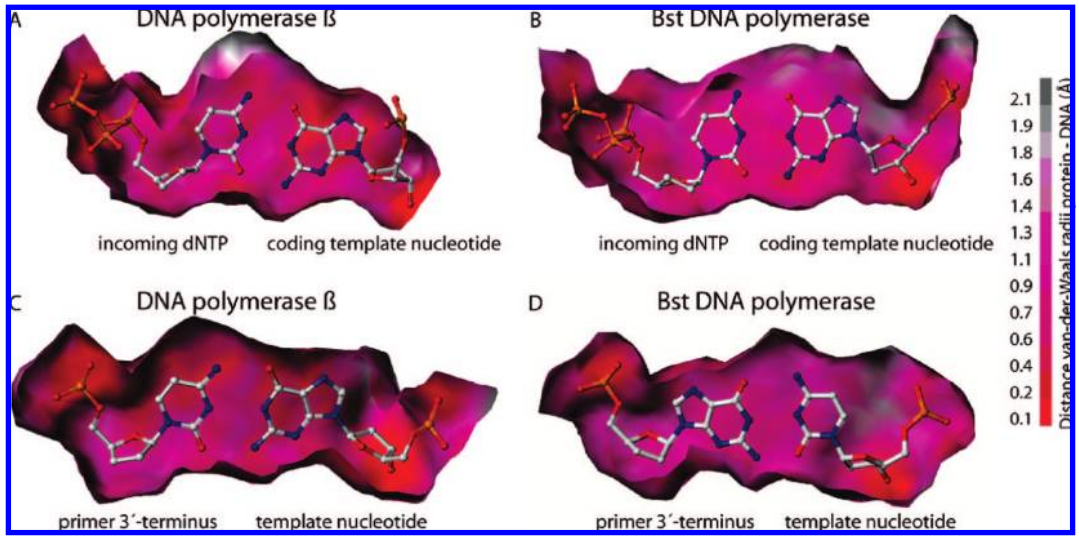

Figure 8. Graphic representations of the distances of the van der Waals radii between DNA and protein for DNA polymerase β and Bst DNA polymerase. The separated surfaces were calculated from PDB-files (Pol β, 1BPY and Bst, 2HVI) using Sybyl 7.2 (Tripos). View of the nascent base pair (incoming and templating nucleotides) for Pol β (A) and Bst Pol (B). Color range is given in the figure. View of the primer terminus and templating base for Pol β (C) and Bst Pol (D).

Overall, Pol β exhibits about 10-fold lower nucleotide insertion fidelity than KF(exo-), which may somewhat vary depending on assay conditions and sequence context.[1d,9a,24] Thus, on the basis of the concept of active site tightness, one would expect a more rigid nucleotide binding pocket in KF(exo-) as compared to Pol β. However, our data obtained with the 4′-alkylated steric probes indicate that additional size of the incoming nucleotide is somewhat better accepted (by a factor of $\sim$5) by the active site of KF(exo-). This indicates more flexible interactions of KF(exo-) with the sugar residue of the incoming nucleotide as compared to Pol β. Thus, the higher nucleotide insertion fidelity of KF(exo-) as compared to Pol β might derive by tighter protein interactions acting on the nucleobase rather than the sugar moiety of the incoming nucleotide, and nucleobase interactions may contribute to nucleotide insertion fidelity to a greater extent in KF(exo-) than in Pol β. Recent experiments in which steric constraints in nucleobase recognition in the active site of KF(exo-) were probed by employment of nucleobase surrogates that gradually expand in steric demand highlight the importance of tight nucleobase fitting to the active site of KF(exo-).[7] It was found that the enzyme's catalytic proficiency as well as fidelity was sensitive to subtle size changes of the nucleobase. However, no such studies concerning Pol β have been reported yet.

When investigating contacts of the enzymes with the 3′-terminal nucleotide of the primer strand, we found that the efficiencies of both polymerases to extend from 4′-alkylated nucleotide differ by several orders of magnitude. While size augmentation by 4′-methylation or 4′-ethylation resulted in a 10- and 15-fold decrease in extension efficiency for Pol β, 7000- and 260 000-fold reductions were observed for KF(exo-). To exclude that the pronounced effect of 4′-alkylation is due to aberrant conformations caused by the modification itself, which might affect enzyme processing in a different way, we conducted NMR investigations to analyze the inherent properties of oligonucleotides bearing 4′-alkylated nucleotides at the 3′-terminus. Little, if any, effect of this chemical modification on oligonucleotide conformation was found. This indicates that for the observed effects size augmentation of the analogues presumably plays the most important role. Crystal structures of Bst Pol[11d,g,h] and Pol β[20] in complex with DNA and dNTP substrates show that both enzymes strongly interact with the 3′-terminal nucleotide of the primer strand. These interactions take place with the sugar−phosphate backbone as well as with the nucleobase (Figure 8). Such interactions were discussed to play important roles in mismatch extension and misalignment fidelity.[1b] Enzymes exhibiting high selectivity are expected to form rigid, nonflexible interactions tolerating fewer deviations, while less selective enzymes are more flexible and may accommodate conformations that allow altered geometries without loosing activity. Perturbation of enzyme substrate interactions by size augmentation at the 3′-terminal primer nucleotide was significantly better tolerated by Pol β than by KF(exo-). While Pol β tolerates size alterations at this position, even subtle size alterations result in a significant drop of KF(exo-) catalytic efficiency. The Bst Pol structures[11d,g,h] as models for KF(exo-) suggest close proximity of the sugar 4′-position to amino acid residues located in the turn of motif C, Val828 and His829 (880 and 881 in KF(exo-), respectively). Both amino acids are located directly nearby the catalytically essential Asp830 (882 in KF(exo-)). Additionally, mutational studies indicate that motif C is important for selectivity.[14a,21,25] It is conceivable that any perturbation at this position (i.e., through size augmentation of the 3′-terminal nucleotide in the primer strand) results in catalytically less proficient enzyme conformations, which in turn causes significantly reduced extension efficiency as observed in our study. In contrast, structures of Pol β suggest a different topology in the near proximity of the sugar 4′-position. The palm domain, which contains β-sheet 5 composed of amino acids Arg253−Pro261,

(23) (a) Minnick, D. T.; Liu, L.; Grindley, N. D. F.; Kunkel, T. A.; Joyce, C. M. *Proc. Natl. Acad. Sci. U.S.A.* **2002**, *99*, 1194. (b) Patel, P. J.; Kawate, H.; Adman, E.; Ashbach, M.; Loeb, L. A. *J. Biol. Chem.* **2001**, *276*, 5044. (c) Shinkai, A.; Patel, P. H.; Loeb, L. A. *J. Biol. Chem.* **2001**, *276*, 18836. (d) Li, S. X.; Vaccaro, J. A.; Sweasy, J. B. *Biochemistry* **1999**, *38*, 4800.
(24) Kunkel, T. A.; Alexander, P. S. *J. Biol. Chem.* **1986**, *261*, 160–166.
(25) Strerath, M.; Gloeckner, C.; Liu, D.; Schnur, A.; Marx, A. *ChemBioChem* **2007**, *8*, 395–401.

contacts the primer end in the minor groove. Arg254 and Asp256 mainly mediate these contacts, which are involved in nucleotidyl transfer. Evidently, our studies indicate that such an enzyme configuration in Pol β is able to accommodate perturbation of substrate interactions significantly better than the one in KF(exo-). With respect to the underlying mechanisms of misalignment fidelity, one would expect that Pol β is superior to KF(exo-) in processing noncanonical substrates and thus exhibits a decreased misalignment fidelity. In fact, this kind of behavior was found as reported earlier by functional investigations of Pol β and KF(exo-).[9] Our results provide first experimental evidence that indeed varied steric constraints act on the 3′-terminal primer nucleotides in both DNA polymerases.

Taken together, for the two polymerases analyzed, Pol β and KF(exo-), we find different steric constraints preferentially acting either on the nucleoside sugar backbone within the active site or on the primer strand. For Pol β, most significant steric effects were found to act on the incoming dNTP, whereas for KF(exo-) primer strand interactions are significantly more pronounced. These findings are in excellent agreement with experimentally derived data concerning the differences in fidelity such as processing of misaligned DNA substrates that cause deletions or insertions and ultimately frameshift mutations. In conclusion, the results presented provide direct evidence for the involvement of considerably varied steric effects on fidelity among different DNA polymerases.

Acknowledgment. We gratefully acknowledge financial support by the Deutsche Forschungsgemeinschaft.

JA8028284